ANTEC® 2021

2021 PROCEEDINGS

CHARACTERIZATION OF POLYPROPYLENE/HYDROCARBON RESIN BLENDS FOR 3D PRINTING

Arit Das, Michael J. Bortner
Department of Chemical Engineering and Macromolecules Innovation Institute, Virginia Tech, Blacksburg, VA

Abstract

Additive manufacturing (AM) of polyolefins, such as polypropylene (PP), employing filament-based material extrusion (MatEx) has gained significant research interest in recent years. The semicrystalline nature of PP makes it challenging to process using MatEx. The addition of amorphous low molecular weight hydrocarbon resins into PP matrix was found to delay the onset of crystallization of the blends. The slow crystallization behavior, as evident by the increased crystallization half-times, aided the relaxation of residual stresses during MatEx of PP blends that resulted in manufactured parts with reduced warpage. Rheological characterizations were performed on the PP blends revealing the shear-thinning nature. The combined interaction among crystallization rates, timescales, and morphology was found to affect the interlayer welding process during MatEx. Mild thermal annealing of the manufactured parts resulted in mechanical properties which approach that of injection molded parts.

Introduction

Additive manufacturing (AM), or 3D printing, is rapidly becoming a potential alternative to traditional subtractive manufacturing techniques such as injection molding [1]. Filament-based material extrusion (MatEx) is one of the most common AM techniques due to the operational ease and low cost associated [2]. MatEx of polymers have gained significant research interest in recent times and printed parts are progressively being used for functional applications in aerospace, automotive, and medical industries [3,4]. Despite the recent advances in MatEx, only a limited number of polymers can be consistently processed using this technique and there is a strong interest in expanding the material catalog.

Semicrystalline thermoplastic polymers such as polyethylene and polypropylene (PP) are an attractive choice for MatEx due to their high demands in consumer and commodity-based applications [5,6]. However, the printed parts of such polymers are invariably associated with a high degree of warpage [7]. This is due to the rapid crystallization behavior of the polymers that leads to residual stress build-up in the printed parts. The highly non-isothermal nature of the printing process coupled with the high thermal gradients exacerbates the problems with printing polyolefins [8]. Moreover, the amount of crystalline content in a printed part directly controls the mechanical properties since increased crystallinity improves part strength as the crystallites can act as physical crosslinks. However, these crystallites can also be detrimental to interlayer chain diffusion by restricting the molecular motion at the interfacial region of two printed layers. Therefore, careful control over the crystallization behavior of polyolefins is desired in order to optimize processing parameters during MatEx.

In this work, the fast crystallization behavior of PP has been arrested by blending it with amorphous low molecular weight hydrocarbon resins. The slower crystallization rate of the blends provided a larger time window for the residual stresses to relax and significantly reduced the issues associated with part warpage during MatEx. The impact of incorporation of the resins on the crystallization behavior, rheological and thermal properties of the blends have been assessed. The mechanical properties and geometric accuracy of the printed parts were characterized. It is postulated the tacky nature of the resin-rich phases in the blends led to improved interlayer adhesion in the printed parts.

Materials and Experimental Methods

Isotactic polypropylene (5E16S), having a melt flow rate of 40g/10min, was obtained from Braskem America, Inc. and two different hydrocarbon resins were obtained from Arkema Chemicals. The hydrocarbon resins had different degrees of hydrogenation; a fully hydrogenated resin (FH) and a partially hydrogenated resin (PH) with a degree of hydrogenation of 98% and 50-60%, respectively were used to prepare the blends with PP. The resins consisted of C5-C9 hydrocarbons and were partially miscible with PP; the extent of miscibility was however dependent on the molecular interactions.

The blends of PP and the hydrocarbon resins at different compositions were prepared in a Brabender Plasticorder mixer. The blending was performed at 170-190°C over a period of 10min at a speed of 32rpm.

Preliminary characterization of the molecular structure and thermal stability of the prepared blends were carried out using Fourier Transform Infra-Red (FTIR) spectroscopy and thermogravimetric analysis (TGA), respectively. FTIR was performed using a Nicolet iS50 spectrometer (Thermo Fisher Scientific Co., USA) n the range of 400–4000 cm^{-1} with a resolution of 4 cm^{-1}. The

FTIR spectra were collected with 128 scans in the absorbance mode. TGA was performed in air from room temperature to 600°C at 10°C/min ramp rate in a TGA 5500 (TA Instruments, USA).

Steady-shear sweeps were performed on compression molded discs of the blends at 180°C in an AR-G2 rheometer (TA Instruments, USA) using a 25mm parallel plate geometry. Crystallization half-times ($t_{1/2}$) were determined using an isothermal crystallization profile at 120°C using Differential Scanning Calorimetry (DSC).

Tensile properties of the printed parts were characterized using an Instron 5944 with a 2 kN load cell at a rate of 3 mm min^{-1}. Printed parts were heat treated at 140°C for 24 h to evaluate the effect of thermal annealing on the tensile properties.

Results and Discussion

Figure 1 highlights the FTIR spectra of PP and its blends with the hydrocarbon resins. For the sake of conciseness, only the compositional extremes (80/20) are presented to gauge the range of expected effect of resin addition. The methylene stretching peak at 2915 cm^{-1} for neat PP loses its intensity slightly upon incorporation of the resins. Similar reduction in the intensity of the methylene deformation peak at 1464 cm^{-1} suggests disruption in crystalline structure of PP [9]. However, the intensity of the methyl peak at 1377 cm^{-1} remains unaltered in the blends compared to neat PP. The results suggest that the overall molecular structure and chemical functionalities of PP is unaltered after resin addition.

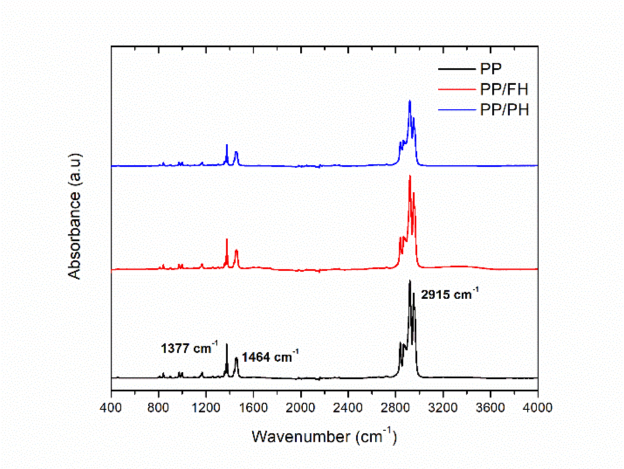

Figure 1. FTIR spectra of PP and 80/20 blends of PP with the two hydrocarbon resins (FH and PH).

The addition of FH and PH resins to neat PP improves the thermal stability of the blends; likely due to the interaction between the resins and PP matrix. The onset degradation temperatures of the 80/20 blends of PP/FH (286°C) and PP/PH (298°C) are higher than that of neat PP (277°C). Upon heating, the hydrocarbon resins undergo side reactions resulting in the formation of a carbonaceous coating on the surface of the blended material [10]. This coating is not prone to oxidation and retards the thermal deterioration process in the PP/hydrocarbon resin blends.

The flow of the polymer melt through a MatEx nozzle is dictated by the shear rates associated with the process. The shear rate can also influence the degree of orientation and stretch of the polymer chains [11]; and can therefore control the crystallization kinetics of the polymer melt post-extrusion through the nozzle during deposition on the print bed. Figure 2 highlights a steady shear rate sweep (0.01-10s^{-1}) performed at 180°C on neat PP and 80/20 blends of PP/hydrocarbon resins. From the log-log shear stress vs. shear rate plot in Figure 2 it is evident that the stresses associated with PP and PP/FH blend are similar to each other that results in almost identical viscosities of the materials. However, the shear stresses for PP/PH blend are higher than that of PP and PP/FH. This suggests that the viscosity of the PP/PH blend is higher; most likely due to increased interaction between the PP matrix and PH resin. From the rheological characterizations, printing parameters can be selected not only to exploit the shear-thinning nature of the polymer melt (enabling extrusion at lower forces due to reduced viscosity) but also to limit the orientation induced effects (by controlling the print speed) that affect the crystallization process [12,13].

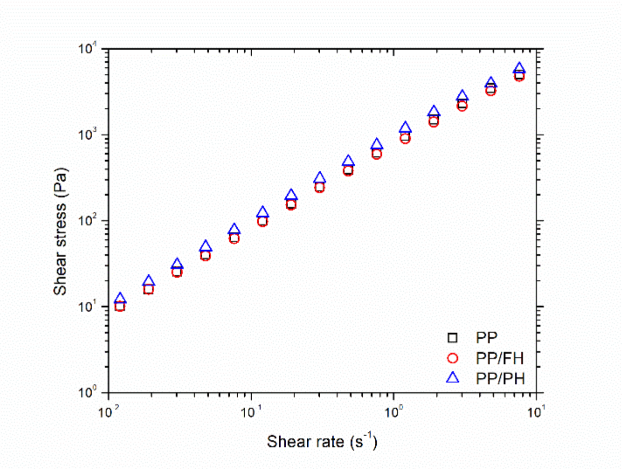

Figure 2. Shear stress versus shear rate profile of PP and 80/20 blends of PP with the two hydrocarbon resins (FH and PH) obtained at 180°C using a 25mm parallel plate geometry in an AR-G2 rheometer.

The crystallization behavior of the PP blends has been characterized by performing isothermal crystallization experiments at 120°C with a hold-time of 10min. The crystallization half-time ($t_{1/2}$), that is a metric of the time required to achieve 50% of the maximum achievable crystallinity, of the blends is approximately 2.5 times that of neat PP, as illustrated in Figure 3. The higher $t_{1/2}$ values indicate retardation of the onset of crystallization in the prepared blends. Increased time spent by the polymer melt prior to crystallization has a direct effect on the printing process. The broader time window allows for increased molecular mobility across the deposited layers as well as assisting with the relaxation of the residual stresses. The degree of crystallinity of the 80/20 blends of PP/FH and PP/PH reduced by 4.5% and 2.5%, respectively as compared to the neat PP.

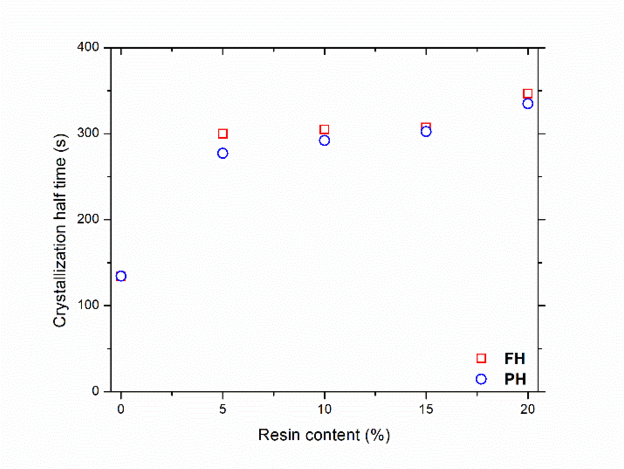

Figure 3. Crystallization halftimes ($t_{1/2}$) of PP and its blends with the two hydrocarbon resins at different compositions.

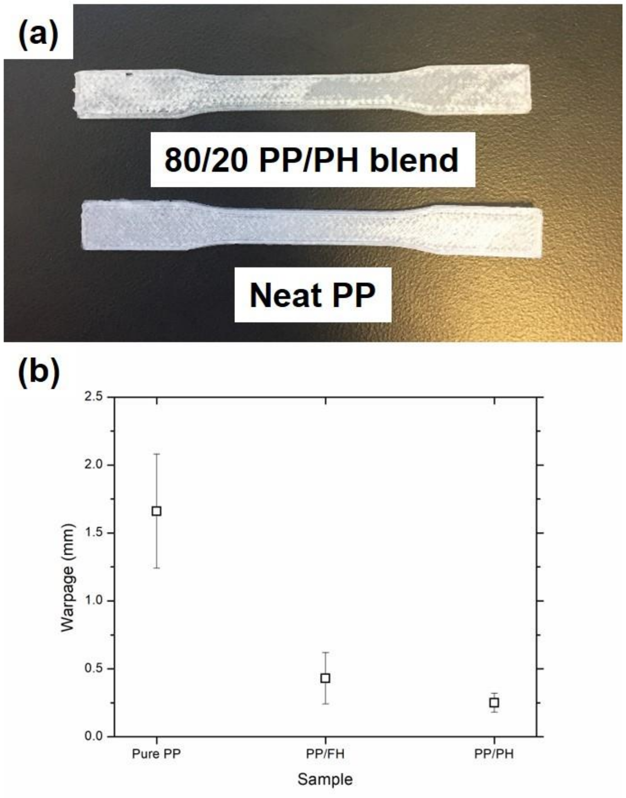

Figure 4. (a) Comparison between a printed PP part and a part printed using 80/20 PP/PH blend; (b) Warpage in the printed parts of PP and 80/20 blends of PP with the two hydrocarbon resins (FH and PH).

The blends of PP/hydrocarbon resins were processed using a single-screw extruder at 190°C to produce 1.75mm filaments for MatEx. Printing experiments were carried out using a Flashforge Creator Pro 3D printer with a 0.4mm nozzle diameter. The print and bed temperature was kept at 180°C and 120°C, respectively. All the parts were printed at 15 mm/s with an infill of 100%. A printed part of neat PP and 80/20 blend of PP/PH resin is presented in Figure 4(a). Printing with the blends results in significant improvements in interlayer as well as bed adhesion. The volumetric shrinkage was determined by comparing the volume of the target print geometry (40mmx 5mm x1mm) to the volume of the printed parts (obtained by measuring the length, width, and thickness of the printed part). The neat PP exhibits a volumetric shrinkage of 18% which significantly reduces to 8.3% and 5.7% for the 80/20 blends of PP/FH and PP/PH resins, respectively. The reduction in shrinkage has a direct effect on limitng the warpage of the printed parts. The warpage in neat PP prints drastically reduces in the prints PP/resin blends, as illustrated in Figure 4(b), and parts with greater dimensional stability are obtained. The better printing performance of the blends was attributed to the polymer melt spending more time in the melt state and hence delaying the onset of crystallization that allowed for better residual stress dissipation.

The tensile properties of the as-printed PP/hydrocarbon resin blends are inferior to that of injection molded PP parts, achieving about 70% of the injection molded properties. In order to improve the properties, the prints were subjected to moderate thermal annealing at temperatures lower than the melting temperature of the blends.

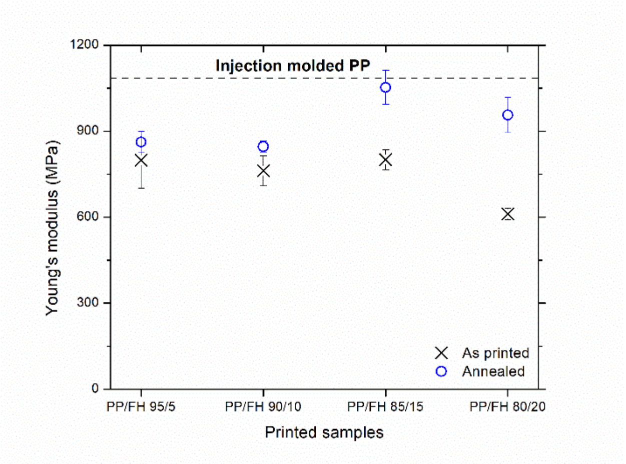

Figure 5. Effect of thermal annealing on the tensile (Young's) modulus of printed parts of the PP/FH hydrocarbon resin blends.

As highlighted in Figure 5, the tensile modulus post-annealing of the printed parts of 85/15 and 80/20 PP/FH hydrocarbon resin blends improved by approximately 32% and 57%, respectively. Such an increase in the tensile modulus values is attributed to enhanced chain diffusion across the interface and better interlayer bonding. Our findings are similar to that reported by previous researchers who investigated the effect of thermal annealing on the mechanical properties of MatEx processed polyphenylene sulfide [14].

Conclusions

PP blended with 20wt% of low molecular hydrocarbon resins was found to improve MatEx processing of the polymer. In terms of mechanical properties of the printed parts, the PP/PH resin blends were superior to the PP/FH blends. The addition of the hydrocarbon resins resulted in slower crystallization kinetics in the PP blends which in turn allows for better stress relaxation and hence reduced warpage in the printed parts. The softer resin domains in the blends result in better interlayer adhesion in the printed parts. Post-printing the parts were subjected to thermal annealing that enhanced the interlayer chain diffusion and resulted in parts that approach >90% of the injection molded properties. The results reported in this work provide the framework for MatEx based manufacturing of semicrystalline polymers in an economical manner.

References

[1] A. Gebhardt, Understanding Additive Manufacturing: Rapid Prototyping, Rapid Manufacturing, and Rapid Tooling. (2011) 40–44.

[2] G.D. Goh, Y.L. Yap, H.K.J. Tan, S.L. Sing, G.L. Goh, W.Y. Yeong, Process–Structure–Properties in Polymer Additive Manufacturing via Material Extrusion: A Review, Critical Reviews in Solid State and Materials Sciences. 45 (2020) 113–133. https://doi.org/10.1080/10408436.2018.1549977.

[3] T.D. Ngo, A. Kashani, G. Imbalzano, K.T.Q. Nguyen, D. Hui, Additive manufacturing (3D printing): A review of materials, methods, applications and challenges, Composites Part B: Engineering. 143 (2018) 172–196. https://doi.org/10.1016/j.compositesb.2018.02.012.

[4] A. Das, C.A. Chatham, J.J. Fallon, C.E. Zawaski, E.L. Gilmer, C.B. Williams, M.J. Bortner, Current understanding and challenges in high temperature additive manufacturing of engineering thermoplastic polymers, Additive Manufacturing. 34 (2020) 101218. https://doi.org/10.1016/j.addma.2020.101218.

[5] M. Spoerk, J. Sapkota, G. Weingrill, T. Fischinger, F. Arbeiter, C. Holzer, Shrinkage and Warpage Optimization of Expanded-Perlite-Filled Polypropylene Composites in Extrusion-Based Additive Manufacturing, Macromolecular Materials and Engineering. 302 (2017) 1700143.

[6] M. Spoerk, J. Gonzalez-Gutierrez, C. Lichal, H. Cajner, G.R. Berger, S. Schuschnigg, L. Cardon, C. Holzer, Optimisation of the Adhesion of Polypropylene-Based Materials during Extrusion-Based Additive Manufacturing, Polymers. 10 (2018) 490. https://doi.org/10.3390/polym10050490.

[7] M. Spoerk, C. Holzer, J. Gonzalez-Gutierrez, Material extrusion-based additive manufacturing of polypropylene: A review on how to improve dimensional inaccuracy and warpage, Journal of Applied Polymer Science. 137 (2020) 48545.

[8] A. D'Amico, A.M. Peterson, An adaptable FEA simulation of material extrusion additive manufacturing heat transfer in 3D, Additive Manufacturing. 21 (2018) 422–430. https://doi.org/10.1016/j.addma.2018.02.021.

[9] J. Li, H. Li, L. Meng, X. Li, L. Chen, W. Chen, W. Zhou, Z. Qi, L. Li, In-situ FTIR imaging on the plastic deformation of iPP thin films, Polymer. 55 (2014) 1103–1107. https://doi.org/10.1016/j.polymer.2014.01.033.

[10] M. Iring, F. Tüdős, Thermal oxidation of polyethylene and polypropylene: Effects of chemical structure and reaction conditions on the oxidation process, Progress in Polymer Science. 15 (1990) 217–262. https://doi.org/10.1016/0079-6700(90)90029-Z.

[11] C. McIlroy, P.D. Olmsted, Disentanglement effects on welding behaviour of polymer melts during the fused-filament-fabrication method for additive manufacturing, Polymer. 123 (2017) 376–391.

[12] C. McIlroy, P.D. Olmsted, Deformation of an amorphous polymer during the fused-filament-fabrication method for additive manufacturing, Journal of Rheology. 61 (2017) 379–397. https://doi.org/10.1122/1.4976839.

[13] C. McIlroy, R.S. Graham, Modelling flow-enhanced crystallisation during fused filament fabrication of semi-crystalline polymer melts, Additive Manufacturing. 24 (2018) 323–340.

[14] E.R. Fitzharris, I. Watt, D.W. Rosen, M.L. Shofner, Interlayer bonding improvement of material extrusion parts with polyphenylene sulfide using the Taguchi method, Additive Manufacturing. 24 (2018) 287–297.